Article

Geometry and Cooperativity Effects in Adenosine–Carboxylic Acid Complexes

Sebastian Schlund, Milena Mladenovic, Eline M. Baslio Janke, Bernd Engels, and Klaus Weisz

J. Am. Chem. Soc., **2005**, 127 (46), 16151-16158• DOI: 10.1021/ja0531430 • Publication Date (Web): 28 October 2005

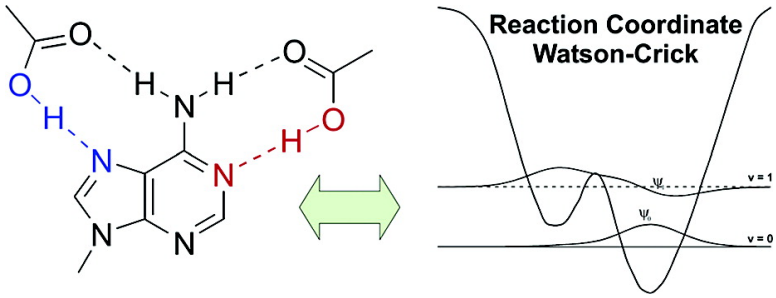

More About This Article

Additional resources and features associated with this article are available within the HTML version:

- Supporting Information
- Links to the 7 articles that cite this article, as of the time of this article download
- Access to high resolution figures
- Links to articles and content related to this article
- Copyright permission to reproduce figures and/or text from this article

View the Full Text HTML

J|A|C|S
ARTICLES
Published on Web 10/28/2005

Geometry and Cooperativity Effects in Adenosine−Carboxylic Acid Complexes

Sebastian Schlund,[†] Milena Mladenovic,[†] Eline M. Basílio Janke,[‡] Bernd Engels,*[,†] and Klaus Weisz*[,§]

Contribution from the Institut für Organische Chemie, Universität Würzburg, Am Hubland, D-97070 Würzburg, Germany, Institut für Chemie, Freie Universität Berlin, Takustr. 3, D-14195 Berlin, Germany, and Institut für Chemie und Biochemie, Ernst-Moritz-Arndt-Universität Greifswald, Soldmannstr. 16, D-17487 Greifswald, Germany

Received May 13, 2005; E-mail: weisz@uni-greifswald.de (experiment); bernd@chemie.uni-wuerzburg.de (theory)

Abstract: NMR experiments and theoretical investigations were performed on hydrogen bonded complexes of specifically 1- and 7-^{15}N-labeled adenine nucleosides with carboxylic acids. By employing a freonic solvent of $CDClF_2$ and CDF_3, NMR spectra were acquired at temperatures as low as 123 K, where the regime of slow hydrogen bond exchange is reached and several higher-order complexes were found to coexist in solution. Unlike acetic acid, chloroacetic acid forms Watson−Crick complexes with the proton largely displaced from oxygen to the nitrogen acceptor in an ion pairing structure. Calculated geometries and chemical shifts of the proton in the hydrogen bridge favorably agree with experimentally determined values if vibrational averaging and solvent effects are taken into account. The results indicate that binding a second acidic ligand at the adenine Hoogsteen site in a ternary complex weakens the hydrogen bond to the Watson−Crick bound carboxylic acid. However, substituting a second adenine nucleobase for a carboxylic acid in the trimolecular complex leads to cooperative binding at Watson−Crick and Hoogsteen faces of adenosine.

Introduction

Hydrogen bond interactions constitute a major driving force in the formation of specific molecular and complex geometries. Thus, protein and nucleic acid secondary and tertiary structural elements as well as many natural and artificial host−guest complexes are partly based on the directive power of intra- and intermolecular hydrogen bond formation.[1,2] In the past, NMR spectroscopic techniques have been established as a powerful tool to study the strength and geometry of hydrogen bonds in both the solid and the liquid state.[3] For the latter, however, NMR signals normally correspond to an average over fast exchanging hydrogen bonded species at ambient temperatures, thus restricting the detailed characterization of hydrogen bonds of individual hydrogen bonded associates.[4] However, employing deuterated freonic mixtures as NMR solvents allows high-resolution NMR spectra to be acquired in the liquid state down to 100 K, where the regime of slow hydrogen bond exchange within the NMR time scale is reached for even weakly hydrogen bonded systems.[5]

We have recently presented low-temperature NMR studies on the binding of an acetic acid ligand to adenosine.[6] Because of its multiple functionalities, this nucleobase can engage in cyclic hydrogen bonds with a carboxylic acid at either its Hoogsteen or Watson−Crick site (Figure 1). In fact, only trimolecular complexes A·HAc_2 (**1a**, Figure 2) and A_2·HAc (**1b**, Figure 2) with both Watson−Crick and Hoogsteen sites of the central adenine base occupied were observed at low temperatures. In all complexes, the acetic acid OH proton is still localized closer to the oxygen of acetic acid in a neutral, nonion pairing complex. Comparing the A·HAc_2 (**1a**) and A_2·HAc complexes (**1b**), the NMR experiment finds a more deshielded

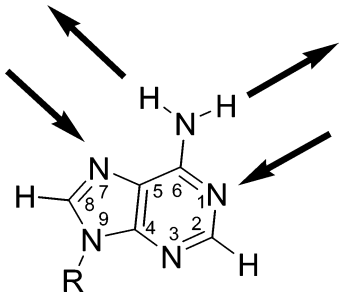

Figure 1. Adenine nucleobase with hydrogen bond donor and acceptor sites at the Hoogsteen (left) and Watson−Crick face (right).

[†] Universität Würzburg.
[‡] Freie Universität Berlin.
[§] Ernst-Moritz-Arndt-Universität Greifswald.

(1) Jeffrey, G. A.; Saenger, W. *Hydrogen Bonding in Biological Structures*; Springer: Berlin, 1994.
(2) Lonergan, D. G.; Deslongchamps, G.; Tomás, S. *Tetrahedron Lett*. **1998**, *39*, 7861−7864.
(3) Hibbert, F.; Emsley, J. *Adv. Phys. Org. Chem.* **1990**, *26*, 255−279.
(4) Iwahashi, H.; Kyogoku, Y. *J. Am. Chem. Soc.* **1977**, *99*, 7761−7765.
(5) (a) Siegel, J. S.; Anet, F. A. L. *J. Org. Chem.* **1988**, *53*, 2629−2630. (b) Golubev, N. S.; Denisov, G. S. *J. Mol. Struct.* **1992**, *270*, 263−276. (c) Weisz, K.; Jähnchen, J.; Limbach, H.-H. *J. Am. Chem. Soc*. **1997**, *119*, 6436−6437. (d) Dunger, A.; Limbach, H.-H.; Weisz, K. *Chem.−Eur. J.* **1998**, *4*, 621−628. (e) Smirnov, S. N.; Benedict, H.; Golubev, N. S.; Denisov, G. S.; Kreevoy, M. M.; Schowen; R. L.; Limbach, H.-H. *Can. J. Chem*. **1999**, *77*, 943−949. (f) Dunger, A.; Limbach, H.-H.; Weisz, K. *J. Am. Chem. Soc*. **2000**, *122*, 10109−10114. (g) Basílio Janke, E. M.; Dunger, A.; Limbach, H.-H.; Weisz, K. *Magn. Reson. Chem*. **2001**, *39*, 177−182.
(6) Basílio Janke, E. M.; Limbach, H.-H.; Weisz, K. *J. Am. Chem. Soc*. **2004**, *126*, 2135−2141.

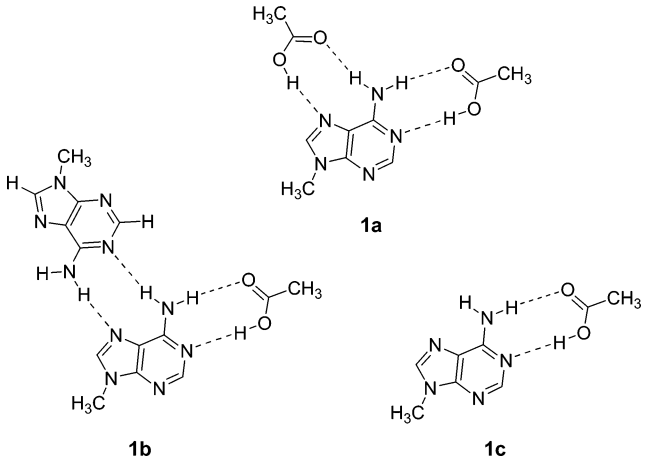

Figure 2. Computed complexes of 9-methyladenine and acetic acid.

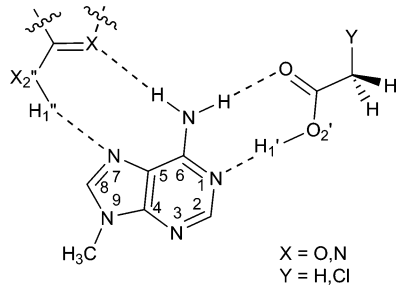

Figure 3. Atom numbering used for the adenine complexes.

proton for the latter in the O−H···N1 hydrogen bridge at the Watson−Crick site (see Figure 3 for atom numbering). For **1a**, the measured value of $\delta(H_{1'})$ is 17.1 ppm, while 17.76 ppm is obtained for **1b**. Obviously, some cooperativity effects arise between Hoogsteen and Watson−Crick binding since the proton chemical shift constitutes a sensitive indicator for the relative hydrogen bond strength.[3,5,7−11] Anticipated cooperativity effects in these higher-order complexes[8,9] and their dependence on the type of ligand[8] are little understood, yet are important not only for the development of adenine receptor molecules that are often based on carboxylic acids[12] but also for a better understanding of interactions within nucleic acids and nucleic acid−protein complexes.[13]

The downfield shift observed in $\delta(H_{1'})$ when going from **1a** to **1b** may result from a displacement of the $H_{1'}$ proton toward the N1 acceptor atom pointing to a strengthening of the hydrogen bond. Such a strengthening of the hydrogen bond is often associated with an elongation of the covalent bond between the hydrogen and the donor. A corresponding example was recently reported by Kar and Scheiner,[8] who investigated cooperative effects in chains consisting of up to five water molecules. For the gas phase, their computations predict an elongation of the covalent OH bond by about 0.003 Å for the donor water molecule positioned at the end of the chain when going from the water dimer to the water trimer. This small change in the geometry was accompanied by a variation of 0.7 ppm in the chemical shift of the bridging hydrogen computed at the equilibrium geometry. Going from the water monomer to the dimer, the variations were 0.006 Å and 2.8 ppm, respectively.

A similar finding was reported by Dingley et al.,[9] who studied cooperative effects in T·A−T and C·G−C triplets and found a strong correlation between the ^{1}H chemical shift of the imino proton and the size of the two-bond scalar coupling across a hydrogen bond $^{2h}J_{NN}$. A similar but inverse correlation is found between the proton chemical shift and the (absolute) size of the covalent $^1J_{HN}$ scalar coupling. On the basis of DFT computations for a model system, they concluded that most of the experimentally observed variations in the parameter are likely caused by changes in the donor−acceptor distances. In this study and in the investigation of Kar and Scheiner,[8] the computed NMR chemical shifts did not include effects resulting from vibrational motions.

The downfield shift could also result from vibrational effects. These effects have been shown to be important for the ^{1}H chemical shift[10,14−16] and were considered in extensive investigations on primary and secondary geometric H/D isotope effects on low-barrier hydrogen bonds performed by Limbach and co-workers. In a series of papers,[10] correlations between ^{1}H chemical shifts and hydrogen bond geometries were studied with the inclusion of vibrationally averaged bond distances allowing for the transfer of chemical shift data into hydrogen bond geometries. Employing empirical corrections for anharmonic zero-point vibrations, these correlations are able to describe isotope effects on hydrogen bond geometries from the weak to the strong hydrogen bond regime, taking into account single- and double-well situations.[10] Isotope effects for intramo-

(7) Kumar, G. A.; Allister, M. A. *J. Org. Chem.* **1998**, *63*, 6968−6972.
(8) Kar, T.; Scheiner, S. *J. Phys. Chem A* **2004**, *108*, 9161−9168.
(9) Dingley, A. J.; Masse, J. E.; Peterson, R. D.; Barfield, J. F.; Grzesiek, S. *J. Am. Chem. Soc*. **1999**, *121*, 6019−6027.
(10) (a) Tolstoy, P. M.; Schah-Mohammedi, P.; Smirnov, S. N.; Golubev, N. S.; Denisov, G. S.; Limbach, H.-H. *J. Am. Chem. Soc*. **2004**, *126*, 5621−5634. (b) Limbach, H.-H.; Pietrzak, M.; Benedict, H.; Tolstoy, P. M.; Golubev, N. S.; Denisov, G. S. *J. Mol. Struct.* **2004**, *706*, 115−119. (c) Smirnov, S. N.; Benedict, H.; Golubev, N. S.; Denisov, G. S.; Kreevoy, M. M.; Schowen, R. L.; Limbach, H.-H. *Can. J. Chem*. **1999**, *77*, 943−949. (d) Benedict, H.; Limbach, H.-H.; Wehlan, M.; Fehlhammer, W.-P.; Golubev, N. S.; Janoschek, R. *J. Am. Chem. Soc*. **1998**, *120*, 2939−2950. (e) Ramos, M.; Alkorta, I.; Elguero, J.; Golubev, N. S.; Denisov, G. S.; Benedict, H.; Limbach H.-H. *J. Phys. Chem. A* **1997**, *101*, 9791−9800. (f) Smirnov, S. N.; Golubev, N. S.; Denisov, G. S.; Benedict, H.; Schah-Mohammedi, P.; Limbach, H.-H. *J. Am. Chem. Soc*. **1996**, *118*, 4094−4101. (g) Benedict, H.; Hoelger, C.; Aguilar-Parrilla, F.; Fehlhammer, W. P.; Wehlan, M.; Janoschek, R.; Limbach, H.-H. *J. Mol. Struct*. **1996**, *378*, 11−16.
(11) (a) Brown, S. P.; Schaller, T.; Seelbach, U. P.; Koziol, F.; Ochsenfeld, Ch.; Klärner, F.-G.; Spiess, H. W. *Angew. Chem., Int. Ed*. **2001**, *40*, 717−720. (b) Ochsenfeld, Ch.; Kussmann, J.; Koziol, F. *Angew. Chem., Int. Ed*. **2004**, *43*, 4485−4489. (c) Fokkens, M.; Jasper, C.; Schrader, T.; Koziol, F.; Ochsenfeld, C.; Polkowska, J.; Lobert, M.; Kahlert, B.; Klärner, F.-G. *Chem.−Eur. J*. **2005**, *11*, 477−494. (d) Ochsenfeld, Ch. *Phys. Chem. Chem. Phys.* **2000**, *2*, 2164−2159. (e) Ochsenfeld, Ch.: Brown, S. P.; Schnell, I.; Gauss, J.; Spiess, H. W. *J. Am. Chem. Soc*. **2001**, *123*, 2597−2606.
(12) (a) Goswami, S.; Hamilton, A. D. *J. Am. Chem. Soc*. **1989**, *111*, 3425−3426. (b) Zimmermann, S. C.; Wu, W. *J. Am. Chem. Soc*. **1989**, *111*, 8054−8055. (c) Adrian, J. C.; Wilcox, C. S. *J. Am. Chem. Soc*. **1989**, *111*, 8056−8057. (d) Conn, M. M.; Deslongchamp, G.; De Mendoza, J.; Rebek, J., Jr. *J. Am. Chem. Soc*. **1993**, *115*, 3548−3557. (e) Alkorta, I.; Elguero, J.; Goswami, S.; Mukherjee, R. *J. Chem. Soc., Perkin Trans. 2* **2002**, 894−898. (f) Castellano, R. K.; Gramlich, V.; Diederich, F. *Chem.−Eur. J*. **2002**, *8*, 118−129.
(13) Pabo, C. O.; Sauer, R. T. *Annu. Rev. Biochem*. **1992**, *61*, 1053−1095.
(14) (a) Benzi, C.; Crescenzi, O.; Pavone, M.; Barone, V. *Magn. Reson. Chem.* **2004**, *42*, 57−67. (b) Golubev, N. S.; Melikova, S. M.; Shchepkin, D. N.; Shenderovich, I. G.; Tolstoy, P. M.; Denisov, G. S. *Z. Phys. Chem.* **2003**, *217*, 1549−1563. (c) Ruden, T. A.; Ruud, K. In *Ro-Vibrational Corrections to NMR Parameters* in *Calculation of NMR and EPR Parameters*; Kaupp, M., Bühl, M., Malkin, V. G., Eds.; Wiley-VCH: Weinheim, Germany, 2004; pp 153−173. (d) Ruud, K.; Astrand, P.-O.; Taylor, P. R. *J. Am. Chem. Soc*. **2001**, *123*, 4826−4833. (e) Sundholm, D.; Gauss, J.; Schäfer, A. *J. Chem. Phys.* **1996**, *105*, 11051−11059.
(15) Stare, J.; Jezierska, A.; Ambrozic, G.; Kosir, I. J.; Kidric, J.; Koll, A.; Mavri, J.; Hadzi, D. *J. Am. Chem. Soc*. **2004**, *126*, 4437−4443.
(16) (a) Munch, M.; Hansen, A. E.; Hansen, P. E.; Bouman, T. D. *Acta Chem. Scand*. **1992**, *46*, 1065−1071. (b) Abildgaard, J.; Bolvig, S.; Hansen, P. E. *J. Am. Chem. Soc.* **1998**, *120*, 9063−9069.

lecular hydrogen bonds were also studied.[17] The influence of vibration anharmonicity was studies by J. Del Bene and coworkers.[18]

Important in this respect are also the extensive investigations of Steiner et al.,[19] who used data of low-temperature neutron diffraction measurements to establish geometric hydrogen bond correlations.

In the present work, we continue our investigations of such cooperative effects in complexes of substituted acetic acid and adenosine as model systems. We include new experimental data for additional compounds, which extend the series in a most appropriate way. Insights into the importance of various effects are obtained by high-level computations, which include solvent effects and account for vibrational effects. Both are found to be extremely important. In addition to providing detailed insights into the contribution of various effects, computations are also used to extend the known series to yet experimentally unaccessible complexes. A critical evaluation of the theoretical approach is enabled by the new experimental data, and the combination of theory and experiment provides for a more detailed and comprehensive understanding of the effects in multiple binding.

Experimental Section

Materials. Reagents of the highest quality available were purchased from Sigma-Aldrich, Deisenhofen, Germany. $^{15}NH_4Cl$ was purchased either from Chemotrade, Leipzig (95% of label), or Deutero GmbH, Kastellaun (99% of label). All reactions were controlled by TLC on silica gel plates (Merck silica gel 60 F_{254}). If necessary, solvents were dried by standard procedures prior to use. The deuterated freon mixture $CDClF_2/CDF_3$ was prepared as described[20] and handled on a vacuum line, which was also used for the sample preparation. 3′,5′-Di-*O*-(triisopropylsilyl)-7-^{15}N-2′-deoxyadenosine and 2′,3′,5′-tri-*O*-(*tert*-butyldimethylsilyl)-1-^{15}N-adenosine were synthesized as described.[6,21−23]

NMR Spectroscopy. NMR experiments were performed on a Bruker AMX500 spectrometer. Temperatures were adjusted by a Eurotherm Variable Temperature Unit to an accuracy of ±1.0 °C. ^{1}H chemical shifts in a freon mixture were referenced relative to $CHClF_2$ (δ_H = 7.13 ppm).

Theoretical Methods. ^{1}H NMR chemical shifts of inter- or intramolecular hydrogen bonds are considerably influenced by vibrational motions.[10,14−16] Additionally, temperature[24] and solvent effects[11] have to be taken into account. The latter may quite strongly affect the proton dynamics.[10,25] To account for the vibrational effects, a two-dimensional treatment, including the high- and low-frequency stretching of the hydrogen bond, would be desirable[15] but requires a two-dimensional potential energy surface. Since we are primarily interested in the trends along a series of molecules, such a treatment would be overly expensive. Moreover, many studies indicate that an effective one-dimensional treatment covers the major effects.[10d,14,16,26] In the present work, we therefore employ an effective one-dimensional treatment to investigate its suitability in explaining the experimental data. To largely include the coupling between the high- and low-frequency stretching of the hydrogen bond, we computed the hydrogen bond stretching potential by relaxing the N−O distance at each point. Within this treatment, we move along the minimum energy path of the two-dimensional surface,[15] thus effectively accounting for the coupling between both motions.

The effective one-dimensional potential for the shuttling motion of $H_{1'}$ between $O_{2'}$ and N1 (for an atom numbering, see Figure 3) was computed employing the B3LYP functional[27] in combination with a TZVP basis set.[28] As described elsewhere, the B3LYP functional in combination with a triple-ζ split valence basis should provide very accurate results for geometries and energies of hydrogen bonded structures.[29] In these computations, all internal coordinates except for the vibrational coordinate were optimized. All computations were performed with the TURBOMOLE program package.[30] Solvent effects are included by using the *Conductor-like Screening Model* (COSMO).[31] Because the dielectric constant of freon solutions varies to some extent depending on temperature and composition, we choose $\epsilon = 40$ as a compromise.[32]

For the present problem, both the O−H [$R(H_{1'}-O_{2'})$] and the N−H [$R(H_{1'}-N1)$] distances of the Watson−Crick hydrogen bond were considered as vibrational coordinates with calculated potentials exhibiting two minima under solvent conditions. In the following, $R_0(H_{1'}-O_{2'})$ and $R_0(H_{1'}-N1)$ represent the equilibrium bond length of the proton covalently attached to oxygen (neutral structure) and to nitrogen (ion pairing structure), respectively. For $R(H_{1'}-O_{2'}) > R_0(H_{1'}-O_{2'})$, the $R(H_{1'}-O_{2'})$ coordinate can serve as the vibrational coordinate, that is, the effective one-dimensional potential can be computed for optimized geometries with fixed $R(H_{1'}-O_{2'})$ values. However, for $R(H_{1'}-O_{2'}) < R_0(H_{1'}-O_{2'})$, a steep repulsive potential and, therefore, an erroneous behavior of the effective potential curve arises because the carboxylic acid molecule would rather dissociate from the adenine base (breaking the O−H···N hydrogen bond) than compressing the OH bond. The dissociation energy amounts to about 30 kJ mol^{-1} (2500 cm^{-1}). This branch of the potential can only be obtained if the NH distance is used as a vibrational coordinate. Since a corresponding problem exists for small NH distances, both potentials have to be merged in order to obtain the full effective potential. In the present paper, the potential with fixed N−H distances is used for the values of the vibrational coordinate larger than 1.25 Å. For those smaller than 1.25 Å, the O−H bond is employed. The correlation given in Figure 4 allows for a better understanding of the relationship between the vibrational coordinate and the actual bond distances. Also, the distances for the computed minima are given in the respective tables.

NMR shielding tensors were calculated on a RHF/TZVP level using the GIAO approach for the gas phase. The relative ^{1}H chemical shifts

(17) (a) Dziembowska, T.; Rozwadowski, Z.; Hansen, P. E. *J. Mol. Struct.* **1997**, *437*, 189−199. (b) Perrin, C. L. *Science* **1994**, *266*, 1665−1668.
(18) (a) Alkorta, I.; Elguero, J.; Mo, O.; Yanez, M.; Del Bene, J. E. *J. Phys. Chem. A* **2002**, *106*, 9325−9330. (b) Del Bene, J. E.; Elguero, J.; Alkorta, I.; Mo, O.; Yanez, M. *J. Phys. Chem. A* **2005**, *109*, 2350−2355.
(19) (a) Steiner, T.; Saenger, W. *J. Am. Chem. Soc.* **1992**, *114*, 7123−7126. (b) Steiner, T.; Saenger, W. *Acta Crystallogr. B* **1994**, *50*, 348−357. (c) Steiner, T. *J. Chem. Soc., Chem. Commun.* **1995**, 1331−1332. (d) Steiner, T. *J. Phys. Chem. A* **1998**, *102*, 7041−7052.
(20) Golubev, N. S.; Smirnov, S. N.; Gindin, V. A.; Denisov, G. S.; Benedict, H.; Limbach, H.-H. *J. Am. Chem. Soc.* **1994**, *116*, 12055−12056.
(21) Ogilvie, K. K.; Thompson, E. A.; Quilliam, M. A.; Westmore, J. B. *Tetrahedron Lett.* **1974**, *33*, 2865−2868.
(22) Gaffney, B. L.; Kung P.-P.; Jones, R. A. *J. Am. Chem. Soc.* **1990**, *112*, 6748−6749.
(23) Gao, X.; Jones, R. A. *J. Am. Chem. Soc.* **1987**, *109*, 1275−1278.
(24) Garcia-Viloca, M.; Gelabert, R.; Gonzalez-Lafont, A.; Moreno, M.; Lluch, J. *J. Am. Chem. Soc.* **1998**, *120*, 10203−10209.
(25) Stare, J.; Mavri, J.; Ambrozic, G.; Hadzi, D. *THEOCHEM* **2000**, *500*, 429−440.
(26) (a) Somorjai, R. L.; Hornig, D. F. *J. Chem. Phys.* **1962**, *36*, 1980−1987. (b) Marechal, Y.; Witkowski, A. *J. Chem. Phys.* **1968**, *48*, 3697−3701. (c) Singh, T. R.; Wood, J. L. *J. Chem. Phys.* **1969**, *50*, 3572−3576. (d) Janoschek, R.; Weidemann, E. G.; Pfeiffer, H.; Zundel, G. *J. Am. Chem. Soc.* **1972**, *94*, 2387−2396.
(27) (a) Becke, A. D. *Phys. Rev. A.* **1988**, *38*, 3098−3100. (b) Lee, C.; Yang, W.; Parr, R. G. *Phys. Rev. B* **1988**, *37*, 785−789.
(28) Schäfer, A.; Huber, C.; Ahlrichs, R. *J. Chem. Phys.* **1994**, *100*, 5829−5839.
(29) (a) Sahu, P. K.; Mishra, R. K.; Lee, S.-L. *J. Chem. Phys. A* **2005**, *109*, 2887−2893. (b) Rabuck, A. D.; Scuseria, G. E. *Theor. Chem. Acc.* **2000**, *104*, 439−448.
(30) Ahlrichs, R. et al. *TURBOMOLE*; Quantum Chem. Group, University of Karlsruhe, Germany, 1988.
(31) (a) Klamt, A.; Schürmann, G. J. *J. Chem. Soc., Perkin Trans.* **1993**, *2*, 799−805. (b) Schäfer, A.; Klamt, A.; Sattel, D.; Lohrenz, J. C. W.; Eckert, F. *Phys. Chem. Chem. Phys.* **2000**, *2*, 2187−2193.
(32) (a) Golubev, N. S.; Denisov, G. S.; Smirnov, S. N.; Shchepkin, D. N.; Limbach, H.-H. *Z. Phys. Chem.* **1996**, *196*, 73−84. (b) Shenderovich, I. G.; Burtsev, A. P.; Denisov, G. S.; Golubev, N. S.; Limbach, H.-H. *Magn. Reson. Chem.* **2001**, *39*, S91−S99.

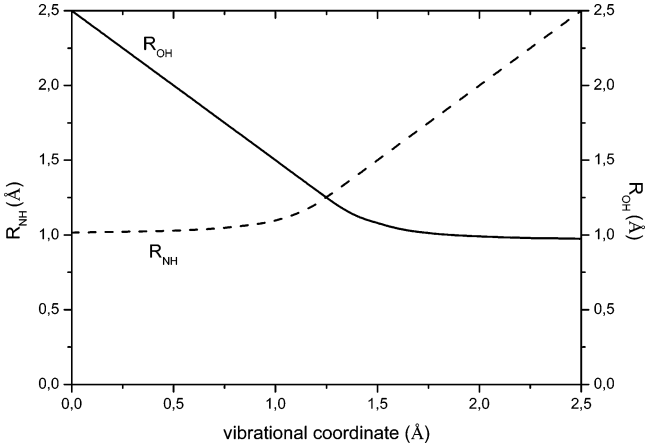

Figure 4. Correlation between the vibrational coordinate and the bond distances, R_{OH} (solid line) and R_{NH} (broken line). All values are given in angstroms.

are calculated with the ^{1}H shielding constant of TMS [$\sigma(H_{TMS}) = 32.257$]. This level was used in various computations of relative ^{1}H shielding constants,[11,33] which showed that the RHF/TZVP approach possesses an accuracy of about 0.2 ppm for relative ^{1}H chemical shifts in most cases. In a recent review,[33b] it was stated that in contrast to the success of DFT in the calculation of molecular structures and energies DFT does not provide a systematic improvement over RHF in the calculation of magnetic shielding constants. Hence, we use DFT only to compute the potential energy surfaces.

To obtain the vibrationally averaged NMR shielding constants, we used the approach developed by Peric et al.[34] For the computation of the reduced mass, μ, the whole motion of the supermolecule has to be considered. Between the minima [$R(H_{1'}-N1) > R_0(H_{1'}-N1)$ and $R(H_{1'}-O_{2'}) > R_0(H_{1'}-O_{2'})$], the reduced mass can be approximated by 1 au because mainly the proton moves. As described above for $R(H_{1'}-O_{2'}) < R_0(H_{1'}-O_{2'})$, the whole carboxylic acid moves away, leading to a flatter potential compared to the OH bond compression. Consequently, for this part of the potential curve, a higher value for the reduced mass had to be taken. A similar problem arises for the part of the potential surface with $R(H_{1'}-N1) < R_0(H_{1'}-N1)$. Test computations employing different reduced masses show, however, that these effects are small. Therefore, a value of $\mu = 1$ au was taken for the whole surface. Temperature effects were taken into account assuming a Boltzmann distribution with $v = 0$ and $v = 1$ vibrational levels. Test calculations show that the influence of the $v = 2$ level is negligible.

Results

NMR Experiments. To investigate adenosine complex geometries and cooperativity effects on ligand binding, we studied the association of adenosine with chloroacetic acid through low-temperature NMR experiments using a freonic solvent in order to reach the slow hydrogen bond exchange regime below 133 K. ^{1}H NMR spectra acquired at 123 K for mixtures of chloroacetic acid (HAcCl) and 2′,3′,5′-tri-*O*-(*tert*-butyldimethylsilyl)-1-^{15}N-adenosine in various stoichiometric ratios are shown in Figure 5. With adenosine in excess, two doublets at 18.67 and 17.64 ppm are observed at low field (Figure 5 top). Employing additional ^{1}H{^{15}N}decoupling experiments, both of these OH protons are unambiguously identified as bound to the adenine Watson−Crick site through their scalar coupling of $J_{NH} \sim 79$ and 85 Hz, with the labeled endocyclic N1 nitrogen. Such large couplings to the nitrogen acceptor atom demonstrate that these protons are mostly transferred to adenine N1 adopting ion pairing species. This is also confirmed by the increase in the J_{NH} scalar coupling for the more upfield shifted resonance and by the corresponding ^{15}N chemical shifts measured with a 2D ^{1}H−^{15}N heteronuclear multiple-quantum coherence (HMQC) experiment at 125 K (see Supporting Information). Thus, more upfield shifted Watson−Crick proton resonances scalar coupled to ^{15}N are correlated with more upfield shifted ^{15}N1 signals as expected for a proton location closer to nitrogen.

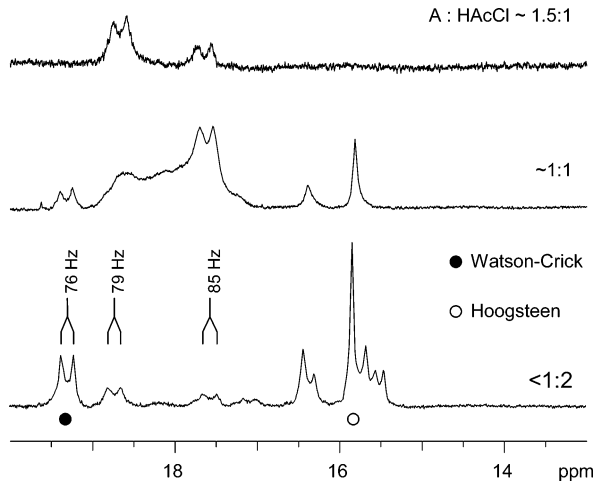

Figure 5. Carboxylic acid OH proton resonances for mixtures of 2′,3′,5′-tri-*O*-(*tert*-butyldimethylsilyl)-1-^{15}N-adenosine and chloroacetic acid with different molar ratios in freon at 123 K. Solid and open circles denote the Watson−Crick and Hoogsteen bound protons, respectively, in a 1:2 A:HacCl complex.

With all of the acid exclusively bound at the adenine Watson−Crick site, the two resonances at low concentrations of chloroacetic acid with stoichiometric ratios of A:HAcCl ~ 1.5:1 can be assigned to 2:1 or 1:1 complexes **2b** and **2c**, respectively (Figure 6). Adding more acid, the situation gets significantly more complex, and an increasing number of signals appear, some of them being significantly exchange broadened at a 1:1 stoichiometric ratio (Figure 5 center). Obviously, with the acid in excess, several different species coexist in solution, making a detailed structural characterization of all the complexes a difficult task. However, protons hydrogen bonded to adenine N1 are easily recognized by their ^{1}H−^{15}N scalar coupling. Information on the more upfield shifted singlet signals comes from 2D NOE contacts observed at 123 K. As expected from their participation in a Watson−Crick hydrogen bond, the ^{15}N scalar coupled signals exhibit NOE cross-peaks to adenine H2. Correspondingly, NOE cross-peaks to adenine H8 identify protons bound to the Hoogsteen face of adenosine. Note that in addition to the absence of a corresponding $^2J_{NH}$ scalar coupling H8 protons of adenosine are easily distinguished from H2 protons by their NOE cross-peaks to sugar protons.[35] In addition, a third type of OH resonances at 15.45 and 15.55 ppm, exhibiting no connectivities to any adenine base protons, must

(33) (a) Gauss, J.; Stanton, J. F. Electron-Correlated Methods for the Calculation of NMR Chemical Shifts. In *Calculation of NMR and EPR Parameters*; Kaupp, M., Bühl, M., Malkin, V. G., Eds.; Wiley-VCH: Weinheim, Germany, 2004. (b) van Wüllen, C. Chemical Shifts with Hartree−Fock and Density Functional Methods. In *Calculation of NMR and EPR Parameters*; Kaupp, M., Bühl, M., Malkin, V. G., Eds.; Wiley-VCH: Weinheim, Germany, 2004. (c) Wang, B.; Fleischer, U.; Hinton, J. F.; Pulay, P. *J. Comput. Chem.* **2001**, *22*, 1887−1895. (d) Wang, B.; Hinton, J. F.; Pulay, P. *J. Comput. Chem.* **2003**, *23*, 492−497. (e) Wang, B.; Hinton, J. F.; Pulay, P. *J. Phys. Chem A* **2003**, *107*, 4683−4687.

(34) (a) Peric, M.; Hachney, M. R. J.; Grein, F. *J. Chem. Phys.* **2000**, *113*, 9011−9021. (b) Peric, M.; Runau, R.; Roemelt, J.; Peyerimhoff, S. D.; Buenker, R. J. *J. Mol. Spectrosc.* **1979**, *78*, 309−332.

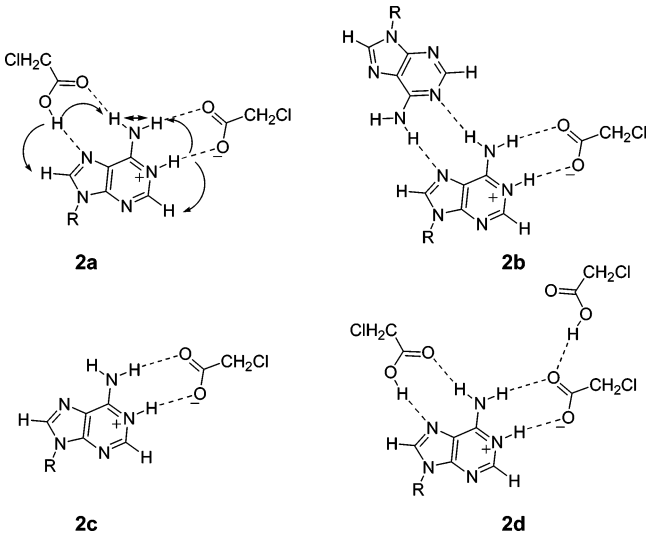

Figure 6. Geometries of complexes formed between adenosine and chloroacetic acid at low temperatures in a freon solvent; arrows in complex **2a** indicate experimentally observed NOE contacts.

Table 1. Summary of the Gas-Phase Computations (structural parameters *d* are given in Å, NMR chemical shifts δ in ppm)

system	d(N···H···O)[a]	vibrational coordinate	$\delta(H_{1'})$
1a	1.707/1.016	1.707	16.20
1b	1.691/1.020	1.691	16.76
1c	1.693/1.019	1.693	16.59
2a	1.668/1.023	1.668	17.41

[a] Left and right numbers refer to the proton−nitrogen and proton−oxygen distance, respectively.

be assigned to protons in a OHO hydrogen bond between two carboxylic acid molecules.

The two resonances at 19.30 and 15.83 ppm, having the same intensity on integration, display NOE contacts to the same amino protons at 11.39 and 9.17 ppm and must be assigned to a 1:2 A·$(HAcCl)_2$ complex **2a** (Figure 6). As is apparent from Figure 5, they are increasingly formed with increasing acid concentration as expected. No attempt was made to assign additional, higher-order complexes that coexist at low temperatures. Interestingly, however, no chloroacetic acid dimers are formed even with an excess of acid, as is evident from comparison with a chloroacetic acid solution at 123 K (δ_{dimer} = 13.15 ppm). Rather, binding of a third acid molecule to form linear aggregates, such as **2d** (Figure 6), may account for the observed most upfield shifted OHO proton resonances at 15.45 and 15.55 ppm (Figure 5 bottom).

Calculations. Results of gas-phase computations on the Watson−Crick hydrogen bond geometry and proton chemical shift $\delta(H_{1'})$ of complexes **1a**−**c** (Figure 2) and **2a** (Figure 6) are summarized in Table 1. In all systems, only the structure with the proton $H_{1'}$ attached to the carboxylate group (neutral structure) represents a minimum. This situation is in agreement with the experimental data for **1a**−**c** but in disagreement for **2a** with its experimentally observed ion pairing structure. The $\delta(H_{1'})$ values computed for the equilibrium structures of **1a**−**c** deviate by about 1.0 ppm from the measured data; that is, despite the agreement in the overall geometrical structure, the deviation between experiment and theory for $\delta(H_{1'})$ is much larger than the expected error bars.[11,33] Nevertheless, while the computed absolute values for $\delta(H_{1'})$ disagree, the difference between **1a** and **b** is nicely reproduced on this level of theory.

If the influence of the freon matrix is taken into account within the framework of the COSMO approach (ϵ = 40), ionic structures in which the proton $H_{1'}$ is bound to N1 rather than to $O_{2'}$ are sufficiently stabilized to become minima (Table 2). For the systems **1a**−**c**, these minima are only 3−5 kJ/mol above the global minimum, which corresponds to the equilibrium structure found for the gas-phase computations (neutral structure). The OH distances increase by only 0.002−0.006 Å in the freon matrix, with the $\delta(H_{1'})$ values computed for the global minima moving toward the measured data. For compound **1a**, it only differs by 0.3 ppm from the experimental value, which is within the range of the expected error bars. For **1b**, the deviation still amounts to 0.8 ppm, being larger than the expected inaccuracy. The computed $\delta(H_{1'})$ values for **1a** and **1b** differ by only 0.1 ppm, that is, at this level, theory cannot explain the difference of nearly 0.7 ppm observed experimentally.

If the influence of the freon matrix is taken into account, theory and experiment agree with respect to the hydrogen bond geometry of compound **2a** since the ion pairing structure becomes the global minimum lying more than 7 kJ/mol below the minimum of a neutral structure. For this ion pairing species, the computed $\delta(H_{1'})$ value is 19.0 ppm, thus only 0.3 ppm lower than the experimental value. This nice agreement supports the expectation that differences between the $\delta(H_{1'})$ values of systems **1a** and **1b** on one hand and **2a** on the other hand result from a proton migration.

The computations also predict two potential minima for the Hoogsteen hydrogen bond to adenine N7 in a freon matrix (not shown). However, with energy differences of 17 (**1a**) and 13 kJ/mol (**2a**), respectively, the influence of these minima is negligible.

For an accurate calculation of proton chemical shifts, an average over the vibrational motions is often necessary.[14] This is also expected for the present systems since $\delta(H_{1'})$ considerably depends on the vibrational coordinate (Figure 7; for a correlation between the vibrational coordinate and the bond distances, see Figure 4). This dependence is also indicated by the shape of the vibrational wave functions, which are exemplarily shown for complexes **1c** and **2a** in Figure 8. A comparison of the various potentials is given in Figure 9. The vibrationally averaged $\delta(H_{1'})$ values are summarized in Table 3. A comparison with the experimentally accessible chemical shifts (Table 4) clearly shows that at this level of theory the values predicted for compounds **1a** and **2a** (T = 128 K) show an excellent agreement with the measured data. To some extent, this excellent agreement is surely fortuitous since the absolute experimental values depend to some extent on the explicit freon composition of the particular sample, which is not accounted for in our theoretical approach. Note, however, that the relative shifts do not depend on the actual composition. For **1b**, the deviation is about 0.3 ppm; that is, all computed $\delta(H_{1'})$ values agree with their experimental counterparts within error bars. This indicates that this computational approach accounts for all important effects (see below).

(35) Wüthrich, K. *NMR of Proteins and Nucleic Acids*; Wiley-Interscience: New York, 1986; pp 205−214.

Table 2. Summary of the Computed Energy Differences ΔE (kJ/mol), Structural Parameters d (Å), and NMR Chemical Shifts δ (ppm) of the Minima for $\epsilon = 40$ (the respective potential curves are given in Figure 8 and in the Supporting Information; the vibrational coordinate is given for comparison)

system	ΔE^a	$\Delta E_1^{\ddagger\, b}$	d(N···H···O)^c	vibrational coordinate	d(N···H···O)^d	vibrational coordinate	$\delta(H_{1'})^e$	$\delta(H_{1'})^f$
1a	5.2	9.5	1.681/1.022	1.681	1.082/1.551	0.949	16.81	20.53
1b	2.8	8.2	1.686/1.022	1.686	1.077/1.572	0.928	16.95	20.08
1c	3.6	8.6	1.683/1.022	1.683	1.075/1.578	0.922	16.87	19.86
2a	7.4	1.9	1.603/1.041	1.603	1.066/1.611	0.889	18.75	19.04

[a] Energy difference between both minima. [b] Barrier height from the minimum in which the proton is attached to the carboxylate group. [c] Structural parameters of the minimum for which the proton is attached to the oxygen. Left and right numbers refer to the proton−nitrogen and proton−oxygen distance, respectively. [d] Structural parameters of the minimum for which the proton is attached to the nitrogen. Left and right numbers refer to the proton−nitrogen and proton−oxygen distance, respectively. [e] NMR chemical shift for the proton attached to oxygen (neutral structure). [f] NMR chemical shift for the proton attached to nitrogen (ion pairing structure).

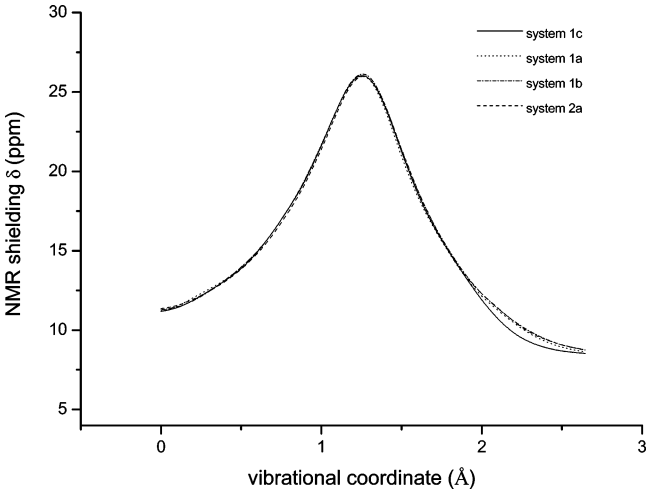

Figure 7. Comparison of the computed relative ^{1}H chemical shifts $\delta(H_{1'})$ along the potential curves for systems **1a**−**c** and **2a**. The computations were performed with the RHF/TZVP ansatz.

Discussion

Low-temperature NMR experiments on adenosine−chloroacetic acid mixtures in aprotic solvents indicate various coexisting higher-order complexes whose formation depends on the acid to adenine base molar ratio. In contrast, previous measurements on various adenine−acid mixtures under fast exchange conditions at ambient temperatures have been interpreted in terms of a simple 1:1 association model, and higher-order complexes have mostly been excluded.[36−38] This might be attributed to the different enthalpic as well as entropic factors that will increasingly favor aggregation to higher-order aggregates at lower temperatures.

The nature of hydrogen bonds can be assessed by NMR spectral parameters, such as ^{1}H NMR chemical shifts or ^{1}H−^{15}N scalar couplings of the proton in the hydrogen bridge. On the basis of our computations (Figure 7), a weakening of the proton−donor bond accompanied by a strengthening of the proton−acceptor bond will give rise to a maximum in the proton chemical shift at about 26 ppm for a centralized proton (neglecting vibrational effects). If the proton is further transferred toward the acceptor atom, the proton chemical shift is predicted to decrease again. Such a proton shift is nicely seen for both Hoogsteen and Watson−Crick hydrogen bonds when going from the 1:2 to the 2:1 adenosine−acetic acid complex

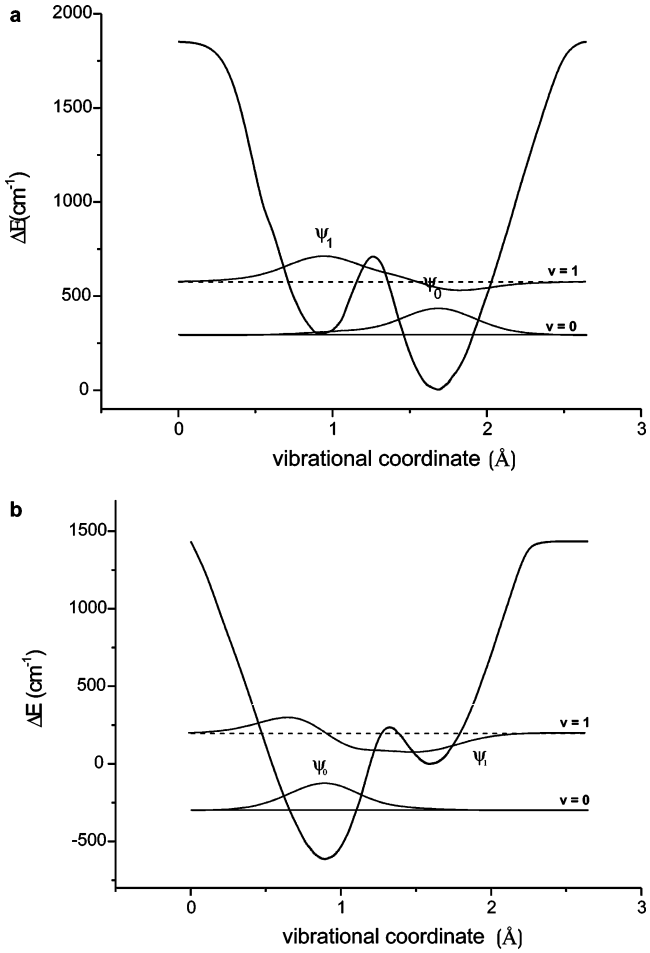

Figure 8. Computed potential curves, energy positions of the vibrational states, and the corresponding wave functions for system **1c** (a) and **2a** (b). The computations were performed with the B3LYP/TZVP ansatz. The minimum on the right-hand side corresponds to a proton close to the carboxyl oxygen.

and finally to the 1:2 adenosine−chloroacetic acid complex, all of which are experimentally accessible. J_{NH} scalar couplings as measured in specifically 1-^{15}N-labeled adenine nucleoside complexes unambiguously point to the formation of neutral complexes with acetic acid (Table 4).[6] In contrast, for chloroacetic acid, the Watson−Crick bound proton is transferred to the nucleobase, forming ion pairing species. Correspondingly, no J_{NH} scalar coupling is observed for Watson−Crick adenosine−acetic acid complexes, whereas a coupling of 76 Hz for the chloroacetic acid 1:2 complex, close to the value expected for a covalent N−H bond with bond order one, indicates an almost complete proton transfer to the N1 acceptor. Interestingly,

(36) Lancelot, G. *J. Am. Chem. Soc.* **1977**, *99*, 7037−7042.
(37) Pistolis, G.; Paleos C. M.; Malliaris, A. *J. Phys. Chem.* **1995**, *99*, 8896−8902.
(38) Rao, P.; Ghosh, S.; Maitra, U. *J. Phys. Chem. B* **1999**, *103*, 4528−4533.

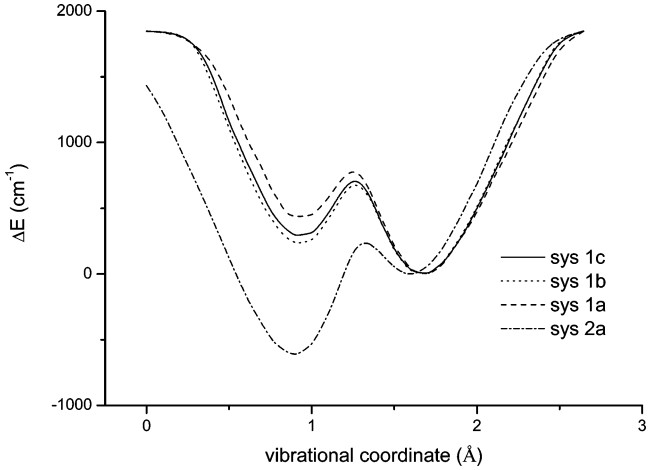

Figure 9. Comparison of the computed potential energy curves. All computations were performed with the B3LYP/TZVP ansatz.

Table 3. Summary of Averaged NMR Chemical Shifts δ (ppm)

	$v=0$		$v=1$			
system	energy[a]	$\delta(H_{1'})$	energy[a]	$\delta(H_{1'})$	Boltz.[b]	$\delta(H_{1'})$, 128 K
1a	301	17.1	691	20.5	0.013	17.2
1b	295	17.9	532	20.1	0.07	18.1
1c	296	17.6	578	20.2	0.042	17.7
2a	316	19.3	809	20.1	0.004	19.3

[a] With respect to the global minimum in cm^{-1}. [b] Boltzmann distribution taking only $v = 0$ and $v = 1$ into account. Test calculations showed a negligible influence of the $v = 2$ levels.

Table 4. Experimental ^1H Chemical Shifts δ (ppm) and J_{NH} Coupling Constants (Hz) of $H_{1'}$ and $H_{1''}$ Protons in Watson–Crick and Hoogsteen Hydrogen Bonds of Adenosine–Acid Complexes

		N1–H–O		N7–H–O	
complex	pK_a (25 °C)	$\delta(H_{1'})$	J_{NH}	$\delta(H_{1''})$	J_{NH}
1a[a]	4.75	17.10	0	15.11	0
1b[a]	4.75	17.76	0		
2a	2.85	19.30	76	15.83	0

[a] Reference 6.

excess chloroacetic acid does not form additional cyclic carboxylic acid dimers but seems to hydrogen bond to the negatively charged carboxylic acid oxygen of the ion pairing associates in a linear fashion. This behavior corresponds to the formation of charge relay chains previously observed between acetic acid (HAc) and pyridine at low temperatures.[10f,20]

Disregarding the N3 endocyclic nitrogen, the adenine base possesses two proton acceptor sites, which can engage in a cyclic hydrogen bond with carboxylic acids, namely, N1 and N7. In water, the pK_a for N1 protonation of adenosine is 3.5, whereas N7 protonation does not take place above pH 1−2. Correspondingly, the hydrogen bond proton is more shifted toward the more basic N1 nitrogen in a Watson−Crick geometry when compared to the N7 in a Hoogsteen geometry. In no cases is a resolved scalar coupling found for N7 bound protons when using a 7-^{15}N-labeled adenine nucleoside; that is, neutral complexes are always formed at the Hoogsteen face.

The differences found in the hydrogen bond geometries of **1a** and **2a** allow for a critical evaluation of the theoretical approach. Indeed, with respect to the geometries of the various complexes, experiment and theory only agree if the influence of the freon matrix is taken into account. By including solvent

Table 5. Summary of the Various Contributions to the Averaged NMR Chemical Shifts δ (ppm) (all computations were performed with $\epsilon = 40$; for more information, see text)

Potential curve from system	NMR values from system	$\delta(H_{1'})$, $v=0$
1a	**1a**	17.12
1a[a]	**1a**	16.92
1a	**1b**	17.37
1b	**1b**	17.90
1b	**1a**	17.64
1b[a]	**1b**	17.46

[a] The average was obtained using a potential curve in which only the minimum with the proton at the carboxylate group was taken into account.

effects, theory predicts a neutral structure for **1a** and **b** and an ion pairing structure for **2a** (see Figure 9). Also, in line with the experiment, theory always finds hydrogens located closer to the oxygen donor within the hydrogen bonds at the Hoogsteen site. In addition to the hydrogen bond geometries, the computed proton chemical shifts also agree well with their experimental counterparts; however, vibrational effects have to be included (Tables 2 and 3).

The good agreement indicates that the employed approach seems to include all important effects. Consequently, theory can also provide an insight into the origin responsible for the trends. Clearly, the differences between **1a** and **b** on one hand and **2a** on the other hand result from a gradual proton transfer induced by the stronger acidity of the chloroacetic acid. For the differences between **1a** and **1b**, however, structural effects seem to be less important. The variations in the equilibrium bond distances when going from **1a** to **1b** ($\Delta R_{O-H} < 0.001$ Å; $\Delta R_{N-H} \approx 0.005$ Å) are small, and for the chemical shifts computed for the equilibrium structures (16.81 vs 16.95 ppm), theory strongly underestimates the experimentally determined difference in $\delta(H_{1'})$ (17.1 vs 17.76 ppm).

An analysis of the various effects is given in Table 5. By combining the potential curve of system **1a** with the NMR shielding curve of system **1b**, a vibrationally averaged $\delta(H_{1'})$ value of 17.37 ppm is obtained. It deviates by 0.25 ppm from the "pure" $\delta(H_{1'})$ value of **1a**, that is, the slight difference in the NMR shielding curve (Figure 7) accounts for 1/3 of the overall effect. The strong influence of the potential curve can be seen from the calculation which combines the potential curve of **1b** with the NMR shielding curve of **1a**, increasing the value of $\delta(H_{1'})$ to 17.64 ppm. This is about 2/3 of the overall effect for $T = 0.0$. The influence of the double-well nature of the potentials of **1a** and **1b** can be seen from the second and the last row of Table 5. If the second minima are omitted, averaged $\delta(H_{1'})$ values of 16.92 (**1a**) and 17.46 ppm (**1b**) are computed. They deviate by 0.2 (**1a**) and 0.4 ppm (**1b**) from the values obtained with the double-well potentials. Assuming a Boltzmann distribution for $T = 128$ K, the value of $\delta(H_{1'})$ increases by about 0.1 ppm for **1a** and 0.2 ppm for **1b** (Table 3).

With vibrationally averaged bond distances $\langle R(N\cdots H)\rangle_{v=0}$, the trends can be explained by changes in the averaged geometries. For **1a** and **1b**, the values amount to 1.6855 and 1.6514 Å, respectively, in line with an effective proton displacement toward the nitrogen acceptor. If the $\delta(H_{1'})$ values for these distances are taken from Figure 7, one obtains $\delta(H_{1'}) = 16.71$ ppm for **1a** and $\delta(H_{1'}) = 17.56$ ppm for **1b**. Using this picture, our model is in line with the findings of Limbach and co-workers.[10f,20]

Due to the importance of solvent effects for the present problem, the question arises whether the used theoretical approach correctly mirrors the physical situation.[39] The adaptation of the environment to changes in the electronic structure of the solute can be divided into polarization effects of the electron shells of the solvent molecules and effects resulting from molecular reorientation (rotation, translation, etc.). While the former will be much faster than the proton transfer process described by the computed double-minimum potentials, the latter (and probably more important ones) will be slower. Thus, the solvent will mainly be adapted to the situation at the global minimum. Going from the global to the local minimum, only a partial adaptation will result in an imperfect orientation of the environment. In contrast, continuum approaches assume a complete reorientation of the surroundings. As a consequence, the computed energy differences between global and local minima are smaller than those in the real situation of a shuttling proton. Correcting for this shortcoming, the importance of the second minima diminishes in **1a** and **1b**, and their influence may even vanish completely (this is even more true for **2a**). This situation is shown by the second and the last row of Table 5, where the second minima have not been taken into account. The computed values for $\delta(H_{1'})$ are 16.92 (**1a**) and 17.46 ppm (**1b**); that is, even in this case, the trend is nicely reproduced and vibrational effects are still the major contributors. Although absolute values deviate more from their experimental counterparts, the agreement is still good considering the uncertainties in experiment and theory.

Clearly, a 1:1 adenosine−acetic acid complex **1c** serves as an important reference for the evaluation of cooperativity effects in binding a second ligand. Unfortunately, such a 1:1 complex was not found experimentally at low temperatures; however, our computations also allow a structural characterization for this bimolecular complex. As shown in Figure 9, binding a second ligand at the adenine Hoogsteen site primarily affects energy differences between minima for the potential curve of the Watson−Crick OH····N hydrogen bond. These effects manifest themselves in a weakening of the H bond and in a shielding of the $H_{1'}$ proton upon binding a second acetic acid at the Hoogsteen site in **1a**. In contrast, a strengthening of the H bond and a deshielding of the $H_{1'}$ proton are calculated upon binding a second adenine base in **1b** (see Table 3). Likewise, an averaged proton position closer to N1 is suggested by a more upfield chemical shift measured in the ion pairing complex **2c** compared to **2a** with a second Hoogsteen bound acid.

These (anti)cooperativity effects can be rationalized in terms of electron-withdrawing and electron-releasing effects exerted by bound ligands. Electron density is expected to gradually decrease in the whole purine ring system upon binding ligands with increasing electron-withdrawing properties. This, in turn, should reduce the acceptor capability of the endocyclic nitrogen with a concomitant shift of the averaged proton location closer to the donor atom. However, when substituting the electron-releasing adenine nucleobase for a Hoogsteen bound second carboxylic acid, the proton is further shifted toward the more potent N1 acceptor, resulting in a downfield or upfield shift in a neutral or ion pairing complex, respectively. Also, binding of a second adenine being essentially basic may even benefit from protonation at N1 and from the concomitant increase in acidity of the exocyclic amino donor.

In the present study, the cooperative effects between N···H−O hydrogen bonds are mediated by the purine ring system. This can be compared to the results of Kar and Scheiner,[8] who investigated the cooperativity in OH···O hydrogen bonds employing chains of water molecules $(H_2O)_n$ up to $n = 5$. Going from $n = 2$ (no additional second ligand) to $n = 3$ (one additional second ligand) corresponds to the changes found between **1c** and **1a**. In their model system, the overall effect is smaller due to the lower acidity of the second ligand. Nevertheless, having a smaller mediating system, the overall effects could be similar. Indeed, based on gas-phase results, this seems to be the case. For the water chain, the covalent O−H bond elongates by about 0.003 Å, that is, the effect is similar to our system with a change in the equilibrium geometry of also about 0.003 Å (Table 1). For the water chain, the computed chemical shift of the bridging hydrogen changes by about 0.7 ppm and is thus comparable to the change of about 0.4 ppm in our system. A comparison of the effects in a solvent is not possible since Kar and Scheiner only discussed the influence of a solvent on binding energies but not on geometries and chemical shifts. Nevertheless, they concluded that the cooperative effects will diminish since the computed binding energies decrease dramatically. As for variations in equilibrium distances, this is indeed found in our study; however, due to vibrational effects, variations in chemical shifts could still be more pronounced.

Conclusion

Chemical shift calculations applying vibrational averaging faithfully reproduce experimental proton chemical shifts in adenosine−carboxylic acid complexes obtained at very low temperatures in the slow hydrogen bond exchange regime. Therefore, geometries on complexes not accessible under the solution conditions employed can be calculated, complementing the available experimental data. On the basis of this combination of experimental and theoretical data, reliable information can be obtained on the strength of individual hydrogen bonds and on the cooperativity of multiple binding to the adenine nucleobase. Clearly, such knowledge is important not only for the design of artificial adenine receptors but also for a better understanding of the many biological interactions involving adenine, such as a component in polymeric nucleic acids or in adenine cofactors.

Acknowledgment. We thank the Deutsche Forschungsgemeinschaft, Bonn-Bad Godesberg, for financial support in the framework of EN197-10/1. We would also like to thank Prof. Dr. M. Perić and Prof. Dr. H.-H. Limbach for valuable discussions.

Supporting Information Available: A section of a $^{1}H-^{15}N$ HMQC spectrum of a 1:2.5 mixture of 2′,3′,5′-tri-*O*-(*tert*-butyldimethylsilyl)-1-^{15}N-adenosine and chloroacetic acid in freon at 125 K. Computed potential curves, energy positions of the vibrational states, and the corresponding wave functions for system **1a** (a) and **1b** (b). This material is available free of charge via the Internet at http://pubs.acs.org.

JA0531430

(39) (a) Searles, D. J.; Huber, H. Molecular Dynamics and NMR Parameter Calculations. In *Calculation of NMR and EPR Parameters*; Kaupp, M., Bühl, M., Malkin, V. G., Eds.; Wiley-VCH: Weinheim, Germany, 2004. A good description of the problems can be taken from ref 10e.